

Mapping Oil in a Coastal Marsh with Polarimetric Synthetic Aperture Radar

Elijah Ramsey III
U. S. Geological Survey
Lafayette, LA, USA
ramseye@usgs.gov

Amina Rangoonwala
Five Rivers Services, LLC
Colorado Springs, CO USA
rangoonwala@usgs.gov

Abstract—Our research focused on the effectiveness of high spatial resolution and fully polarimetric L-band SAR (NASA Uninhabited Aerial Vehicle SAR [UAVSAR]) for mapping oil in wetlands, specifically during the Macondo-1 oil spill and its impacts within Barataria Bay in eastern coastal Louisiana. Oil detection relied on PolSAR decomposition and subsequent classifications of the pre-spill (2009) and post-spill (2010) single look complex (SLC) scenes and numerous site observations. Results found that observed shoreline marsh structural damage accompanied by oil occurrence were evident as anomalous features on post-spill but not on the pre-spill SLC flight line data and that these nearshore features were reflected as a change in dominant scatter in Freeman-Durden (FD) and Cloude-Pottier (CP) decompositions and Wishart classifications seeded with the FD and CP classes. Pre- and post-spill SLC data and all decompositions and classifications also revealed a class of interior marshes within the central core of the study region that was associated with a transform of dominant scatter mechanism. The change of dominant scatter is associated with a preponderance of evidence that supports the penetration of oil-polluted waters into interior marshes. Contrary to documented nearshore impacts, however, the lack of contemporaneous observational data and possible shallow flooding in the pre-spill marsh prevent absolute determination of whether UAVSAR detected oil occurrences in the interior marshes.

Index Terms—Oil, Marsh, Remote Sensing, Multi-polarization, Radar, Decomposition, Classification

I. INTRODUCTION

During the Deepwater Horizon (DWH) oil spill, which occurred between 20 April and 15 July 2010, $4.4 \times 10^6 \pm 20\%$ barrels of crude oil entered the Gulf of Mexico (GOM) waters [1]. Even though most of this oil never reached the expansive saline-to-freshwater wetlands of the GOM, many marsh wetlands were impacted to some extent by oil from the spill. Although specific details of the wetland response cannot be predetermined, oil contamination is often detrimental to marsh health [2]. In order to determine whether or not wetland change is caused by a toxic spill, subtle changes in the wetland condition must be detectable; however, in a dynamic coastal wetland it is often difficult to clearly identify the root cause of change [3]. The most immediate and direct connection between the oil spill and degradation of coastal wetlands is the known spatial occurrence and duration of oil exposure. The

advent of a remote sensing system capable of mapping oil in the marsh near to the time of the spill could provide a clearer spatial association between latent changes observed in the marsh and oil occurrences [e.g., 3].

Mapping oil on the open water is accomplished with either optical or radar imaging; however, in vegetation canopies these remote sensing technologies have not been effectively demonstrated. Outside of weather constraints primarily affecting optical collections, dense wetland-canopy structures can limit the use of optical-wavelength sensors and short-wavelength radars for determining the occurrence of oil on the plants and ground at the subcanopy level [3, 5]. In the marsh, the influences on the radar backscatter dominantly depend on (1) the distribution and content of water in the vegetation and soil and (2) canopy structure [4, 5]. Injection of oil with dramatically different dielectric properties than water at the microwave wavelengths could alter the radar backscatter signature providing the means to detect the presence of oil in the marsh and soil.

High variability in canopy structure suggests that a multi-polarization or polarimetric SAR (PolSAR) sensor may be better suited than one with single polarization because the additional information can be used to better differentiate changes in backscatter that are caused by natural variation in marsh structure [5] from those caused by the presence of oil. In addition, the use of L-band radar ensures that the polarimetric backscatter information reflects the entire marsh canopy structure and underlying background, as well as surface properties. This enhanced polarimetric information improves the potential to detect and differentiate subtle alteration of bulk-canopy dielectric properties caused by the presence of oil coating the plant stems and leaves and sediment from changes in canopy structure.

II. DATA AND METHODS

Data from pre- and post-spill Uninhabited Aerial Vehicle SAR (UAVSAR) flights over Barataria Bay, Louisiana (Fig. 1) were used to determine whether changes in polarimetric backscatter can be linked to oil occurrences as a coating on some portion of the plants or soil surface. The UAVSAR is an airborne, fully polarimetric, L-band SAR system that provides for the complete characterization of the scattering field in the

recorded intensities and phases of the HH (horizontal send and receive), VV (vertical send and receive), and cross (HV and VH) polarization backscatter. Precision repeat-track capability (5-m position accuracy) enables direct comparison between revisit data collections [6]. A more detailed account of the processing and analyses methods including multiple look directions and a more complete discussion of the results is contained in Ramsey et al. [7].

A. Assessing Signal to Noise Influences

To ensure correct interpretation of products derived from data analyses, we compared HV backscatter intensities of marshes, ponds and tidal creeks, and Barataria Bay waters located in the near- to far-range of the flight lines to noise intensities obtained from Jones et al. [6]. Comparisons showed that with the possible exception of minor land covers (e.g., mud flats), products output from the polarimetric decompositions associated with marshes are fully interpretable [7]. On the other hand, in oiled waters where backscatter intensities were near the noise floor, the interpretation was limited to identification of change; decompositions were not directly interpretable in oiled waters [7].

B. Flight Line Locations and Timings

From the June 2010 UAVSAR campaign of the entire U.S. GOM, we chose a single Mississippi River Delta (MRD) post-spill flight line and a replicate pre-spill flight line collected 17 June 2009 (Fig. 1). The southeast-to-northwest pre- and post-spill flight lines included our study region in northeastern Barataria Bay where satellite tracking showed large oil slicks had already spread prior to the 2010 UAVSAR campaign and where field observations confirmed extensive shoreline impacts. Data from the 2009 and 2010 MRD flight lines provide the basis for our pre- and post-spill comparison and detection of abnormal backscatter change unrelated to marsh growth stage and related to oil from the DWH.

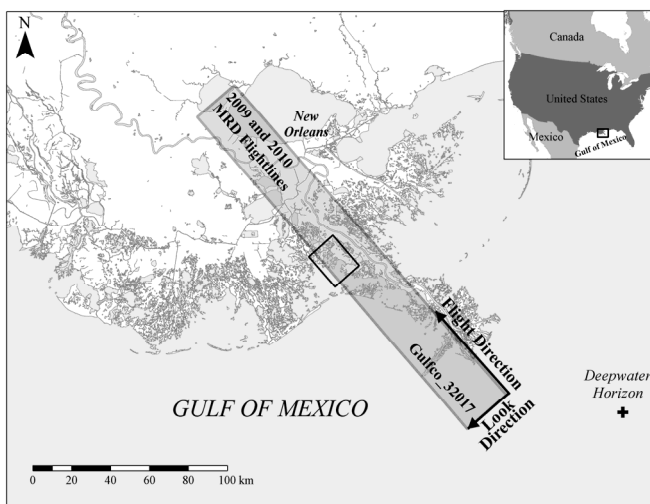


Fig. 1. UAVSAR flight lines collected on 17 June 2009 (pre-spill) and replicated on 23 June 2010 (post-spill) in both flight track and radar operation. Arrows depict the flight and look directions. The black box represents the study area described in this paper. Adapted from Ramsey et al. [7].

C. Field and Satellite Observations

1) Shoreline Observations

On 23 June 2010, the day of the UAVSAR overflight, a field support crew documented oil occurrences extending 2-4 m along shorelines within the northeastern portion of Barataria Bay (e.g., Fig. 2). In addition to these shoreline observations, we used maps produced from Shoreline Cleanup Assessment Techniques (SCAT) documenting levels and locations of shoreline oil impacts [8]. SCAT-produced maps document oil occurrences at the Barataria Bay entrance on 19 May 2010, severe shoreline oil-impacts on 11 June 2010, most notably in the northeast of Barataria Bay, and the existence of extensive shoreline oil-impacts throughout Barataria Bay on 25 June 2010, two days following the UAVSAR overflight.

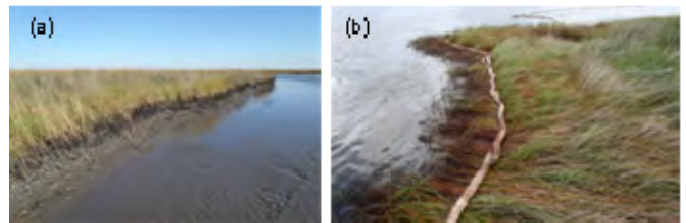


Fig. 2. (a) Oil on lower plant canopy in an interior marsh. (b) Shoreline damage associated with oil impact. Boom washed onto marsh during persistent high tides.

2) Satellite Oil Tracking and Inland Water Level

NOAA maps document that the extensive oil slick on 23 May 2010 had spread far into the interior of the bay by 4 June 2010 impacting marshes at Barataria Bay's northeast extent (Figs. 3(a,b)) [9]. Although no observations are available for the interim periods, it is likely that oil-laden waters persisted inside Barataria Bay and were moved about by prevalent winds and tides from 23 May 2010 onward.

During the time that oil slicks covered large portions of Barataria Bay, persistent northerly winds produced sustained high waters (Figs. 4a and b) that drove oil containment booms up into the marsh (see Fig. 2b). These sustained northerly winds that likely resulted in the northward expansion of oil laden waters into the study region also likely led to the prolonged marsh flooding by these oil laden waters. Extensive shoreline impacts in the study area were first documented on 11 June 2010 just after this period of persistent northerly winds and elevated water levels [7].

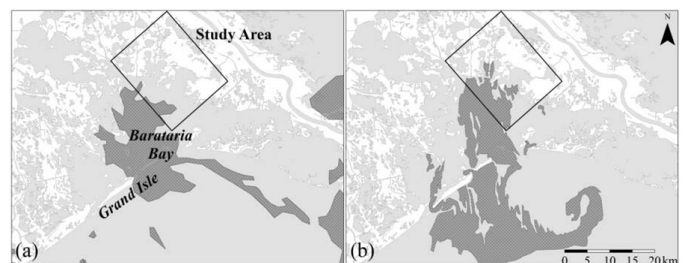


Fig. 3. Extensive oil slicks in Barataria Bay, Louisiana, derived from satellite observations on (a) 23 May 2010 and (b) 4 June 2010 [7]. The box outlines the study area.

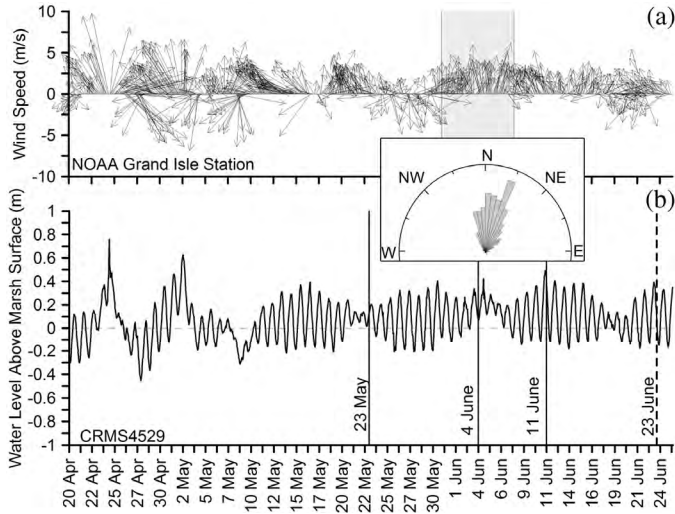


Fig. 4. (a) Wind vectors recorded at the entrance of Barataria Bay [10]. (b) The inland hydrograph [11] begins at the 20 April 2010 DWH explosion and ends after the 23 June 2010 UAVSAR overflight [7]. The wind rose plot between (a) and (b) shows the dominant winds towards the north-northeast during the sustained high water event (highlighted in grey on (a)).

D. UAVSAR Data Analyses

1) Single-Look Complex Post-Collection Processing

We used single-look complex (SLC) calibrated radar cross sections from UAVSAR, which are posted at a spacing of 0.6 m (azimuth) and 1.6 m (slant range), with a processing resolution of 1.0 m in azimuth and 1.6 m in slant range [7]. Each pixel in the SLC data file contains the amplitude and phase of the electromagnetic wave measured by the four channels of the PolSAR sensor, representing the four complex elements of the scattering matrix [6], which relates the incident (transmit) to the scattered (receive) electric field. In order to apply polarimetric decomposition to determine the scattering mechanism, the scattering matrix elements were transformed into multivariate distributions represented by the polarimetric covariance matrix. A non-overlapping 7 by 3 pixel boxcar filter was applied to the data to reduce the speckle noise [12, 13] and produce a multilooked (MLC) complex data with pixels 4.2 m by 4.8 m in azimuth and range, respectively [14], and an effective number of looks of twelve.

2) PolSAR Decomposition and Classification

We extracted information about the marsh physical properties from the four complex polarimetric backscatter components of the SLC data (e.g., [12, 15, 16]) by using the standard Freeman-Durden (FD) and the Cloude-Pottier (CP) decomposition and unsupervised classification methods [7, 17–18]. These decompositions provided quantifiable methods for determining change that should relate directly to changes in the marsh structure and properties. Even though improvements and some drawbacks have been noted in the application of these polarimetric decomposition methods as applied to natural target scattering (e.g., [12, 15, 16, 19]), these methods are widely used, operationally available, and proven useful (e.g., [12, 15, 16, 19, 20, 21]).

The FD decomposition method applies a physical model based on randomly oriented, thin cylindrical dipoles, first-order Bragg surface scatter, and a double-bounce scattering from a dihedral corner reflector to determine the fractions of volumetric (random), surface, and double-bounce scattering exhibited in each target [12, 15, 17, 19]. In solving for the backscatter mechanism fractions, volumetric scatter is related directly to HV backscatter [17].

The CP decomposition method applies eigenvector decomposition to describe the average or dominant scattering mechanisms of each target [12, 18, 21]. Four eigenvalues were used to calculate the scattering entropy— H , the non-polarized power— A , and the average scattering mechanisms— α (surface scattering $\alpha=0^\circ$, volumetric scattering, $\alpha=45^\circ$, dihedral scattering $\alpha=90^\circ$) [12, 13, 18].

The Wishart classification uses a maximum likelihood approach based on the complex Wishart distribution. Although it is not based on the physics of the scattering mechanism, the Wishart classification utilizes the full range of complex polarimetric information [22] and has increased the interpretability of the landcover classifications when seeded with prior unsupervised classifications [12, 19, 20, 21] such as provided by either FD or CP decompositions.

III. RESULTS

A. Inundation Influences on the 2009 and 2010 SAR Backscatter

The presence or absence of inundation is the highest frequency environmental change in these coastal marshes. Marsh water levels recorded in the study region [11] at the times of the 2009 and 2010 UAVSAR overflights showed the water level to have been 7–9 cm higher in 2009. To ascertain whether this difference in water level substantially influenced the radar backscatter, the difference of the 2009 and 2010 HH-polarization intensity was calculated across the entire Barataria Bay marshes in the MRD flight lines [e.g. 23]. Differences between -2 to +2 dB dominated the marsh landscape demonstrating high and extensive temporal and spatial uniformity of marshes surrounding Barataria Bay. Differences <-2 dB in the northeast of the study region indicate possible shallow flooding in 2009; however, the restricted area encompassing these higher differences does not suggest pervasive flooding existed in the study region that would negate the interpretability of the pre- and post-spill comparative analyses [7].

B. Freeman-Durden Decomposition and Classification

Volumetric scatter was the dominant, roughness the secondary, and double-bounce the minor backscatter mechanisms exhibited in the 2009 pre-spill FD classification (Fig. 5). Inspection of the 2009 pre-spill and 2010 post-spill FD classifications indicated that many marshes lying interior to a shoreline with documented oil impacts exhibited a change

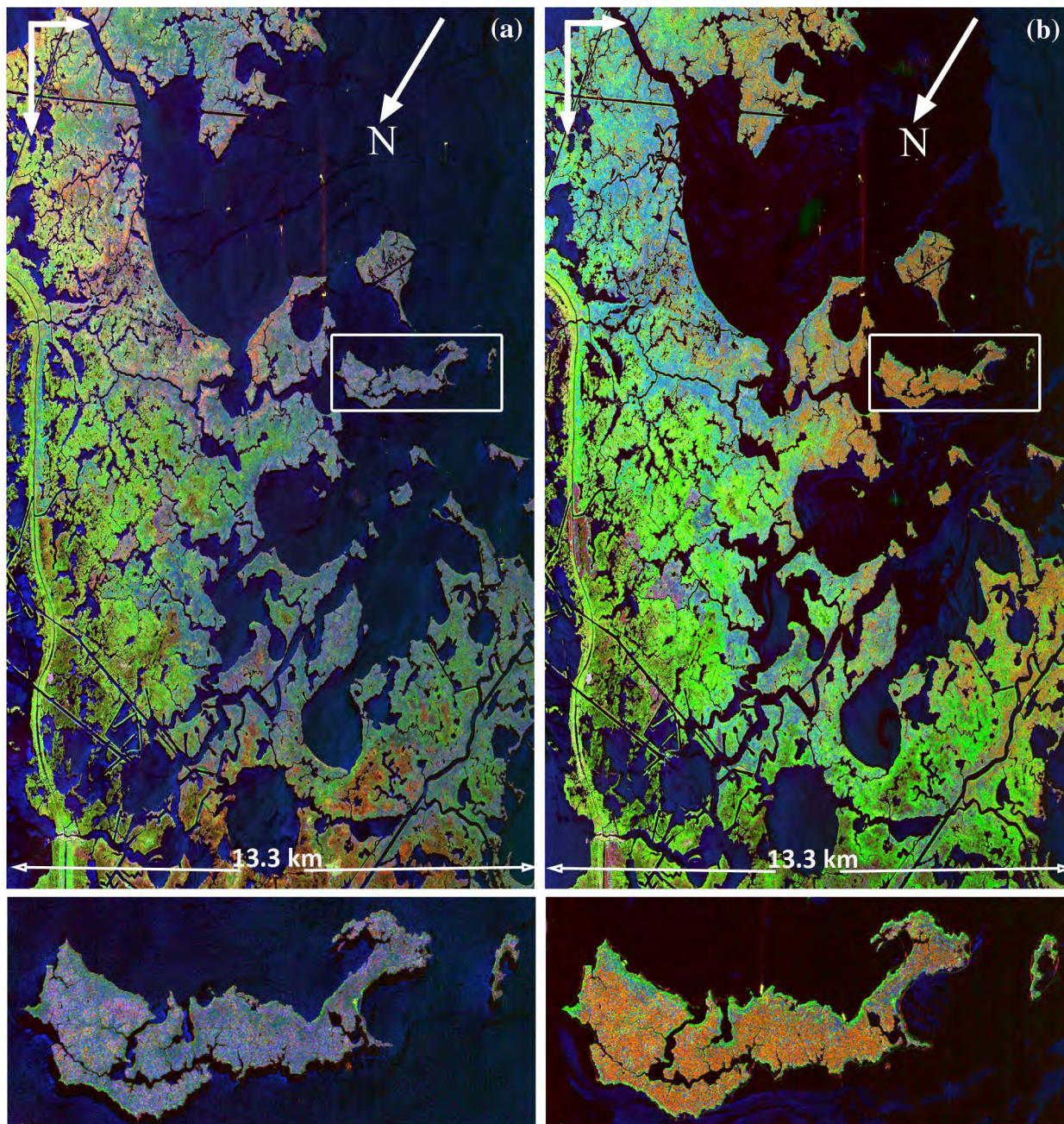


Fig. 5. FD decompositions of the 2009 (a) and 2010 (a). Colors depict dominant fractions of surface (blue), volumetric (green), and double-bounce (red) backscatter. The same color reference table was used in 2009 and 2010 renditions. Adapted from Ramsey et al. [7].

in the dominant backscatter mechanism. In some cases these interior marshes, which had in 2009 exhibited roughness and, in some cases, volumetric backscatter mechanisms, exhibited a dominant double-bounce scattering mechanism in the 2010 post-spill FD decomposition. Locations of the marshes spatially exhibiting this change in scattering mechanism coincided with locations of the anomalous spectral changes observed in the 2009 and 2010 MLC intensity data of the MRD flight lines [7]. In contrast to the interior marshes, the dominant backscattering behavior of features associated with shoreline oil impact changed from “roughness” in the 2009 FD

decomposition to “volumetric scattering” in the 2010 FD decomposition. The shore-normal widths of these nearshore-change features could range from 20 m to 40 m, extending inland far beyond the visually observed 2- to 4-m shoreline area of oil-related marsh damage. As in the MLC intensity data, the FD-classified nearshore-change features coincided well with evidence of shoreline oil occurrences [7].

C. Cloude-Pottier Decomposition and Classification

The CP decomposition classifications produced 16 classes representing different Entropy-Alpha-Anisotropy categories

(see [7]). Lower class variability and higher spatial uniformity in the marshes was exhibited in the 2009 pre-spill CP classification than the 2010 post-spill CP classification. Higher variability in the post-spill CP classification chiefly was due to the addition of a CP class that aligned with prominent changes in the interior marsh reflected in the pre- and post-spill MLC data of the MRD flight lines. These prominent changes primarily exhibited a change, between 2009 and 2010, from low and moderate entropy to low entropy, from high and low anisotropy to low anisotropy, and from low alpha (surface roughness) to dominantly high alpha (double or even dihedral scatter) and some midlevel alpha volumetric (dipole) scatter [7]. Although still dominantly associated with surface roughness, the CP classification exhibits an increase in volumetric scatter associated with nearshore marshes that include severe shoreline impacts [7].

D. Wishart-Freeman-Durden Supervised Classification

Initiated with the per-pixel roughness, double-bounce, and volumetric-input fractions in the FD classification, the Wishart classification that can produce up to nine classes, produced two classes each for the roughness and double-bounce, and three class for the volumetric backscatter mechanisms (Figs 6(a,b)). For the central core of the study region, the 2009 and 2010 Wishart-FD classification largely mimicked prominent changes produced in the 2009 and 2010 FD decompositions (Fig. 5(a,b)). In oil-impacted areas of the 2010 MRD flight line, marshes that exhibited predominantly rough surface scattering behavior in 2009 were associated with double-bounce scatter dominance in the 2010 post-spill Wishart-FD classification. Scattering dominance associated with nearshore marshes with observed severe oil-impact switched from a surface roughness-dominant mechanism to a volumetric-scatter mechanism between 2009 and 2010 (from Class 3 to Class 9). The water classification changed between 2009 and 2010 to include a second water class associated with surface-oil. This change is associated with the radar power return being reduced to near the instrument noise floor by oil damping the surface waves.

E. Wishart-Cloude-Pottier Supervised Classification

The pre-spill Wishart-CP classification initiated with 16 CP classes displayed higher class variability and lower spatial uniformity than exhibited in the pre-spill and post-spill CP decompositions and classifications (see [7]). The post-spill Wishart-CP classification contained two marsh classes centered within the area of observed oil occurrence. Their combined spatial distribution resembled the distinctive changes exhibited in the 2010 MLC intensity data [7]. In effect, the Wishart-CP classification recreated one marsh class

indicative of oil occurrence largely similar to classes created with the FD, Wishart-FD, and CP decompositions and classifications, and a second class that extended the first oil-related marsh class into interior marshes displaying abnormal change in the post- and pre-spill MLC intensity data.

IV. DISCUSSION AND CONCLUSION

Pre-spill and post-spill fully polarimetric L-band SAR data were analyzed to assess their effectiveness to detect oil occurrences in wetlands, including oil coating plant stalks and soil in the lower marsh canopy. Predominant differences in the pre- and post multilooked (MLC) PolSAR data represented oiled surface waters, damaged shoreline marshes, and backscatter changes within marshes in the vicinity of the impacted shorelines. These anomalous features identifiable in the post-spill MLC intensity data that were not identifiable in the pre-spill MLC intensity data provided the first evidence that oil occurrences within marshes are distinguishable with PolSAR data [7].

Along with direct interpretation of the MLC intensity data, we used Freeman-Durden (FD) and Cloude-Pottier (CP) decompositions of the MLC data to determine the physical basis for the abnormal changes observed in the MLC data and to provide a less subjective and more consistent and operational method to map the extent of oil intrusion into wetlands. Both FD and CP decompositions identified shoreline marshes of confirmed oil-spill impact and exhibited a change in backscatter from dominantly surface to primarily multiple-bounce (double or even number) in interior marshes that were likely to have been in contact with oil-laden waters. CP decomposition indicated that the pre- to post-spill change in interior marshes was accompanied by an increasing dominance of a single backscatter mechanism.

The Wishart-FD classification simplified the continuous FD decomposition-classification by compactly reproducing each FD dominant backscatter mechanism as two to three discrete classes. This restriction of the Wishart-FD classification led to a high spatial correspondence between FD and Wishart-FD classification maps. Even though Wishart-CP and CP classes were not directly relatable as were Wishart-FD and FD classes, interior marshes that likely experienced oil impact were highlighted in the post-spill CP as well as in post-spill Wishart-CP classification [7]. In contrast to the Wishart-FD and FD close replication, the Wishart-CP classification increased the detail of the original CP classification; however, the increase in interpretability of the Wishart-CP classifications was less clear. A weakness of the Wishart-CP classification was its sensitivity to changes in the input variance and look angle [7].

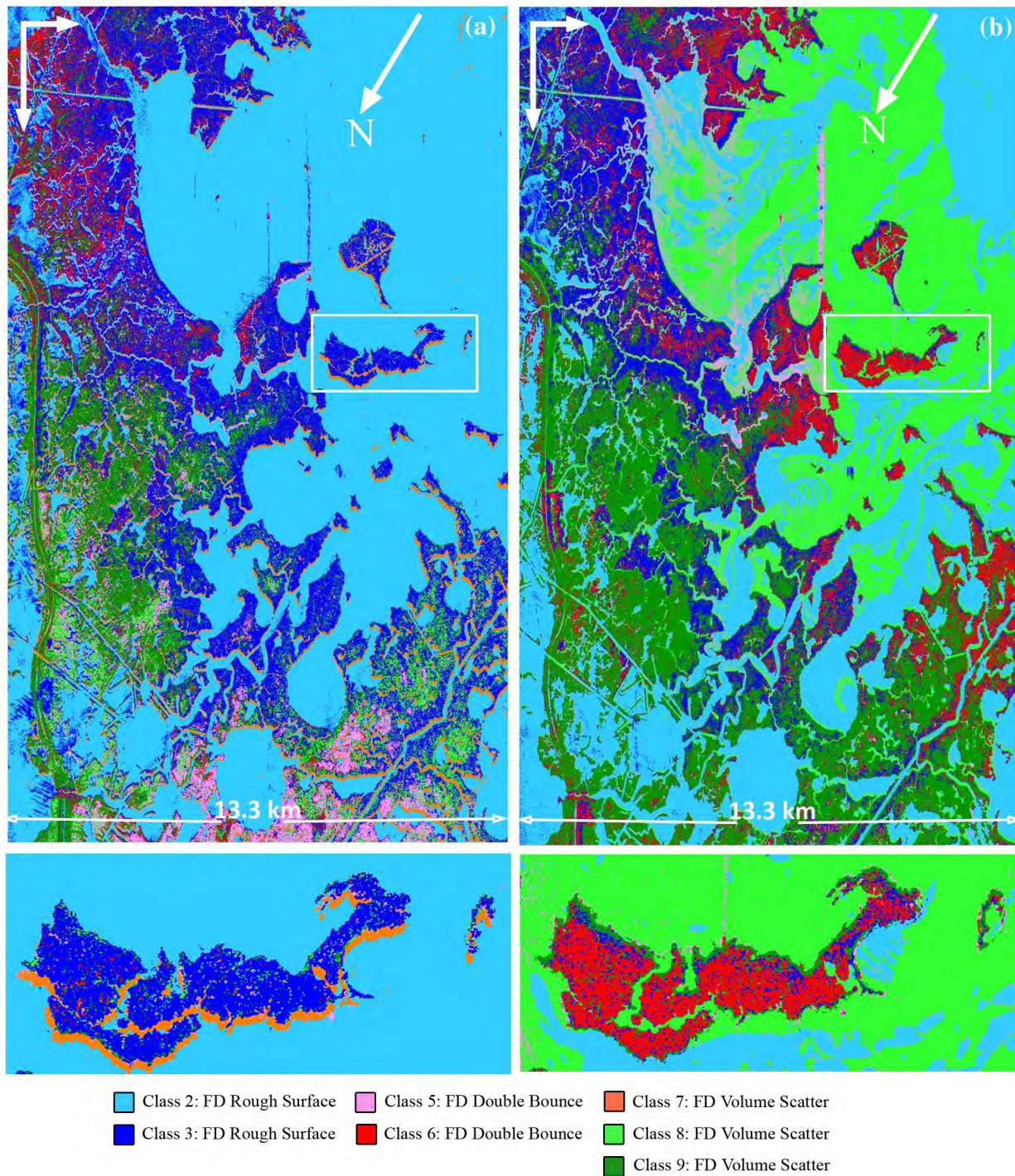


Fig. 6. Results of the Wishart classification initiated with FD classes (see Fig. 5) of the 2009 (a) and 2010 (b). Note the wind-shadow water class (7) on the 2009 inset. The same color reference table was used in the 2009 and 2010 renditions. Adapted from Ramsey et al. [7].

Ground-based observations documented a mix of shoreline oil impact severities most often incorporating canopy structure damage with an oil coating. These shoreline impacts clearly visible 2-4 m into the shoreline marsh were dramatically exhibited in comparison between pre- and post-spill PolSAR-based products. However, in marshes butting heavily oiled

shorelines, these features could extend up to 40 m into the adjacent marsh in the decomposition and classification products. This inland extension supports limited ground-based evidence that the PolSAR data can be used to detect subcanopy oil in the marsh without accompanying canopy structural damage.

REFERENCES

As for PolSAR-based detection of oil occurrences in interior marshes, reasonable evidence exists for the spatial extension of oil occurrence from the nearshore into the farther interior marsh. The concurrence and juxtaposition of persistent onshore winds, prolonged marsh flooding, and extensive oil-laden waters in the study area, the dramatically impacted shorelines, and the protective booms washed into the nearshore marsh support penetration of oil into the interior marshes, even if the flood waters carried only thin surface films of oil. Possible shallow flooding in the pre-spill flight line and the lack of direct observational data within the interior marsh, however, prevent confirmation that backscatter changes in the interior marshes were associated with oil coating plant stalks and sediment.

The most important result of this research is confirmation that UAVSAR detected both shoreline damage and oil occurrences in the vicinity of impacted shorelines and that these impacts and occurrences were reproduced in backscatter decompositions and in the classifications based on those decompositions. These results confirm that low-noise, high-spatial resolution, PolSAR can be used to identify marsh areas affected by oil slicks and can be used to inform design of future satellite-based instruments for fine-scale wetland ecosystem monitoring.

ACKNOWLEDGMENT

We thank Francis Fields Jr. of the Apache Louisiana Minerals LLC, a subsidiary of Apache Corporation, for access to their properties and Jeff Deblieux IV of the Louisiana Land and Exploration Company, a subsidiary of Conoco Phillips, for access to their properties. We thank Buddy Goatcher of the U.S. Fish and Wildlife Service (USFWS) and Warren Lorentz of the U.S. Army Corps of Engineers for allowing the use of the helicopter video-survey imagery. We thank Robert Gosnell of the USFWS for access to the Southwest Louisiana National Wildlife Refuge Complex and Guthrie Perry of the Louisiana Department of Wildlife and Fisheries for access to the Rockefeller State Wildlife Refuge. We acknowledge the support of Kara Holekamp, Philip Kuper, and Steve Tate of the Stennis Space Center, Darin Lee of the Louisiana State Office of Coastal Protection and Restoration, and Bruce Davis of the Department of Homeland Security, who collected the ground-site data in Barataria Bay during the UAVSAR overflights. Gratitude is extended to Dirk Werle of Aerde Environmental Research and Kevin Jones of PCI Geomatics for their thoughtful reviews and to Connie Herndon of U.S. Geological Survey. The research described in this paper was carried out in part at the Jet Propulsion Laboratory, California Institute of Technology, under a contract with the National Aeronautics and Space Administration. Mention of trade names or commercial products is not an endorsement or recommendation for use by the U.S. Government.

- [1] T. J. Crone and M. Tolstoy, "Magnitude of the 2010 Gulf of Mexico oil leak," *Science*, vol. 330, p. 634, 2010.
- [2] C. Hershner and J. Lake, "Effects of chronic oil pollution on a salt-marsh grass community," *Mar. Biol.*, vol.56, pp. 163-173, 1980.
- [3] E. Ramsey III, D. Werle, Y. Suzuoki, A. Rangoonwala and Z. Lu, "Limitations and Potential of Optical and Radar Satellite Imagery to Monitor Environmental Response to Coastal Emergencies in Louisiana, USA," *J. Coastal Res.*, vol. 28(2), pp. 457-476, 2012.
- [4] E. Ramsey III, "Remote sensing of coastal environments," in *Encyclopedia of Coastal Science, Encyclopedia of Earth Sciences Series*; Schwartz M. L., Ed. Springer: Dordrecht, Netherlands, 2005, pp. 797-803.
- [5] E. Ramsey III, G. Nelson, S. Sapkota, S. Laine, J. Verdi and S. Krasznay, "Using multiple polarization L band radar to monitor marsh burn recovery," *IEEE Trans. Geosci. Remote Sens.*, vol. 37(1), pp. 635-639, 1999.
- [6] C. E. Jones, B. Minchew, B. Holt, and S. Hensley, "Studies of the Deepwater Horizon Oil Spill with the UAVSAR Radar," in *Monitoring and Modeling of the Deepwater Horizon Oil Spill: A Record-Breaking Enterprise*, vol.195, American Geophysical Union Monograph Series: Washington, DC USA, 2011, pp. 33-50.
- [7] E. Ramsey III, A. Rangoonwala, Y. Suzuoki, and C. E. Jones, "Oil detection in a coastal marsh with polarimetric SAR," *Remote Sens.*, vol. 3, pp. 2630-2662, 2011.
- [8] Shoreline Cleanup Assessment Techniques (SCAT) maps, Available: http://gomex.erma.noaa.gov/layerfiles/4809/metadata/cumulative_scat_houma.htm; accessed 1 September 2011.
- [9] NESDIS Anomaly Analysis. NOAA Satellite and Information Service, Available: <http://www.nesdis.noaa.gov/>; accessed 1 September 2011.
- [10] NOAA Meteorological Data, NOAA, NOS/CO-OPS (National Ocean Service/Center for Operational Oceanographic Products & Services) Available: <http://tidesandcurrents.noaa.gov/gmap3/>; accessed 1 September 2011.
- [11] SONRIS (Strategic Online Natural Resources Information System). Available: http://sonris-www.dnr.state.la.us/www_root/sonris_portal_1.htm; accessed 10 December 2010.
- [12] J-S. Lee and E. Pottier, "Polarimetric Radar Imaging: From Basics to Applications (Optical Science and Engineering)," CRC Press: Boca Raton, FL, USA, 2009.
- [13] S. Cloude and E. Pottier, "A review of target decomposition theorems in radar polarimetry," *IEEE Trans. Geosci. Remote Sens.*, vol. 34(2), pp. 498-518, 1996.
- [14] PCI Geomatics, "Geomatica SPW 10.1 User Guide (SAR Polarimetry Workstation)," PCI Geomatics Enterprises, Inc.: Richmond Hill, Ontario, Canada, 2007.
- [15] J. dos Santos, I. Narvaes, P. Graca and F. Goncalves, "Polarimetric responses and scattering mechanisms of tropical forest in the Brazilian Amazon," in *Advances in Geoscience and Remote Sensing*; Jedlovec, G., Ed. InTech: Vukovar, Croatia, 2009, pp. 183-206.
- [16] R. Touzi, A. Deschamps and G. Rother, "Phase of target scattering for wetland characterization using polarimetric C-band SAR," *IEEE Trans. Geosci. Remote Sens.* vol. 47(9), pp. 3241-3261, 2009.
- [17] A. Freeman and S. Durden, "A three component scattering model for polarimetric SAR data," *IEEE Trans. Geosci. Remote Sens.*, vol. 36, pp. 963-973, 1998.

- [18] S. Cloude and E. Pottier, "An Entropy based classification scheme for land applications of polarimetric SAR," *IEEE Trans. Geosci. Remote Sens.*, vol. 35(1), pp. 68–78, 1997.
- [19] C. Putignano, "PolSOM and TexSOM in Polarimetric SAR Classification," Tor Vergata University, Department of Computer, Systems and Production Engineering GeoInformation: Rome, Italy, Ph.D. Thesis, 2009, p. 163.
- [20] J-S Lee, M. Grunes, T. Ainsworth, L. J. Du, D. Schuler and S. Cloude, "Unsupervised Classification Using Polarimetric Decomposition and the Complex Wishart Classifier," *IEEE Trans. Geosci. Remote Sens.* vol. 37(5), pp. 2249–2258, 1999.
- [21] M. Ouarzeddine, B. Souissi and A. Belhadj-Aissa, "Unsupervised classification using Wishart classifier," in *Proceedings of the 3rd International Workshop on Science and Applications of SAR Polarimetry and Polarimetric Interferometry*, Frascati, Italy, 22-26 January, ESA Communication Production Office: Paris, France, 2007.
- [22] A. Nielsen, K. Conradsen and H. Skriver, "Polarimetric Synthetic Aperture Radar Data and the Complex Wishart Distribution," in *13th Scandinavian Conference on Image Analysis (SCIA)*, Series Lecture Notes in Computer Science 2749, J. Bigun and T. Gustavsson, Eds. Springer: Berlin, Germany, 2003, pp.1082-1089.
- [23] E. Ramsey III, Z. Lu, Y. Suzuoki, A. Rangoonwala and D. Werle, "Monitoring duration and extent of storm surge flooding along the Louisiana coast with Envisat ASAR data," *IEEE Trans. Geosci. and Remote Sens.*, vol. 4(2), pp. 387–399, 2011.